

Partial Information Rate Decomposition

Luca Faes,^{1,2,*} Laura Sparacino,¹ Gorana Mijatovic,² Yuri Antonacci,¹
Leonardo Ricci,³ Daniele Marinazzo,⁴ and Sebastiano Stramaglia⁵

¹*Department of Engineering, University of Palermo, Palermo, Italy*

²*Faculty of Technical Sciences, University of Novi Sad, Serbia*

³*Department of Physics, University of Trento, Italy*

⁴*University of Ghent, Belgium*

⁵*University of Bari Aldo Moro and Istituto Nazionale di Fisica Nucleare, Sezione di Bari, Italy*

(Dated: February 21, 2025)

Partial Information Decomposition (PID) is a principled and flexible method to unveil complex high-order interactions in multi-unit network systems. Though being defined exclusively for random variables, PID is ubiquitously applied to multivariate time series taken as realizations of random processes with temporal statistical structure. Here, to overcome the incorrect depiction of high-order effects by PID schemes applied to dynamic networks, we introduce the framework of Partial Information Rate Decomposition (PIRD). PIRD is formalized applying lattice theory to decompose the information shared dynamically between a target random process and a set of source processes, implemented for Gaussian processes through a spectral expansion of information rates, and demonstrated in practice analyzing time series from large-scale climate oscillations.

Keywords: partial information decomposition, mutual information rate, coarse graining, lattice theory

The pursuit of assessing and disentangling complex many-body interactions in network systems composed by multiple connected units is crucial to data-driven research in many scientific fields. In this context, partial information decomposition (PID) constitutes a comprehensive framework designed to understand how information is distributed in multivariate systems [1]. The goal of PID is to decompose the information that a "target" random variable shares with a set of "source" variables into components highlighting how such an information is distributed among the sources: the *unique* information that is exclusively available from each source, the *redundant* information that can be obtained from at least two different sources, and the *synergistic* information that is revealed only when multiple sources are considered simultaneously. This framework has gained popularity as a main tool to assess high-order interdependencies from network datasets collected in several applicative fields of physics, engineering, biology, and artificial intelligence [2–7].

Even though the PID is specifically defined for random variables, the data sequences over which it is computed are often multivariate time series that can only be regarded as realizations of random processes. In this case, under the implicit underlying assumption that the processes at hand are stationary and memoryless (i.e., composed by independent and identically distributed (i.i.d.) variables), the PID decomposes the information shared instantaneously by the processes. However, the i.i.d. assumption is typically not tested in practice and is often violated in applications of information decomposition where the analyzed data exhibit temporal correlations [8–10]. Here, we warn against the use of PID in processes exhibiting evident temporal statistical structure, showing that the presence of temporal correlations has a profound impact on the multivariate information shared at lag zero by multiple random processes (Fig. 1). On the other hand, applications of the PID to time-lagged variables selected ad-hoc from the

processes (e.g., [5, 11, 12]) are inherently focused on specific portions of the system dynamics, thus revealing the lack of general and comprehensive approaches to information decomposition that can provide a full account of the dynamical nature of random processes. The present work fills this fundamental gap by formalizing the PID framework for networks of stationary random processes, leveraging the use of entropy rates as basic elements of information decomposition.

We start considering the information-theoretic measure quantifying the overall degree of association between two (possibly vector) discrete-time random processes $X = \{X_t\}_{t \in \mathbb{Z}}$ and $Y = \{Y_t\}_{t \in \mathbb{Z}}$, which is the mutual information rate (MIR) [13] defined as the limit

$$I_{X;Y} = \lim_{n \rightarrow \infty} \frac{1}{n} I(X_1, \dots, X_n; Y_1, \dots, Y_n), \quad (1)$$

where $I(\cdot; \cdot)$ denotes the mutual information (MI) between two random variables. Then, considering X as composed by N source processes, $X = \{X_1, \dots, X_N\}$, and denoting Y as target process, we exploit the mathematical lattice structure defined for the PID [1] and apply it to represent the set-theoretic intersection of multiple processes, so as to decompose the MIR as

$$I_{X;Y} = \sum_{\alpha \in \mathcal{A}} I_{X_\alpha;Y}^\delta, \quad (2)$$

where $X_\alpha \subset X$ groups the source processes indexed by α , and \mathcal{A} is the collection of all subsets of sources such that no subset is a superset of any other (e.g., $\mathcal{A} = \{\{1\}\{2\}, \{1\}, \{2\}, \{12\}\}$ if $N = 2$) [1]. Eq. (2) achieves a so-called *partial information rate decomposition* (PIRD) whereby the MIR is expanded as the sum of contributions (information rate atoms $I_{\cdot;\cdot}^\delta$) identified by the lattice structure. Moreover, the marginal MIR terms involving any individual source process X_i are constructed additively by summing the information rate of the atoms positioned at the level $\{i\}$ and downwards in the lattice according to

$$I_{X_i;Y} = \sum_{\beta \preceq \{i\}} I_{X_\beta;Y}^\delta, \quad i = 1, \dots, N \quad (3)$$

* Correspondence email address: luca.faes@unipa.it

where \preceq identifies precedence based on the partial ordering imposed by the lattice structure [1]. As happens with PID, the consistency equations (2) and (3) do not suffice to solve the PIRD problem because they provide a number of constraints lower than the number of information rate atoms to be computed (i.e., $N + 1 < |\mathcal{A}|$). Thus, to complete the PIRD it is necessary to define a so-called *redundancy rate* function, here denoted as I_{\cdot}^{\square} , which generalizes the MIR over the lattice. The redundancy rate extends (3) to each atom $\alpha \in \mathcal{A}$, fulfilling

$$I_{X_{\alpha};Y}^{\square} = \sum_{\beta \preceq \alpha} I_{X_{\beta};Y}^{\delta}. \quad (4)$$

Then, once the redundancy rate is known, the information rate associated to all atoms can be retrieved via Möbius inversion of (4). When $N = 2$ source processes are considered, the PIRD atoms identify the redundant, unique and synergistic information rates (respectively, $R_{Y;X} := I_{X_{\{1\}\{2\}}^{\delta};Y}$, $U_{Y;X_1} := I_{X_{\{1\}}^{\delta};Y}$ and $U_{Y;X_2} := I_{X_{\{2\}}^{\delta};Y}$, and $S_{Y;X} := I_{X_{\{12\}}^{\delta};Y}$), while for $N > 2$ such contributions may result from coarse-graining approaches that sum the information rate of multiple atoms [4]. Being explicitly defined for random processes, the PIRD defined by (2,4) generalizes previous approaches applying PID to random variables arbitrarily selected from the processes: in the absence of temporal correlations, the PIRD reduces to the static PID decomposing the instantaneous information shared by the processes, $I(X_t; Y_t)$; in the case of strictly causal processes with the target not sending information to the sources, it reduces to the PID applied to the joint transfer entropy from all sources to target, $T_{X \rightarrow Y} = I(X_{<t}; Y_t | Y_{<t})$ ($X_{<t} = \lim_{k \rightarrow \infty} (X_{t-k}, \dots, X_{t-1})$) [14].

The operationalization of the function needed to capture the notion of redundancy rate can follow several different strategies proposed to define redundancy among random variables. These strategies differ depending on the philosophy followed to satisfy the desired properties (e.g., decision-, game-, information-theoretic), on the nature (continuous or discrete) of the analyzed variables, and on assumptions made about their distribution (e.g., Gaussian) [1, 15–18]. A popular approach is to define redundancy as the ensemble (time-domain) average of a given *local* redundancy measure obtained elaborating properly computed pointwise MI values [16, 19]. Here we follow a conceptually similar approach, making it specifically tailored to random processes in that (i) it is applied to MIR instead of MI and (ii) it is implemented through a local representation in frequency rather than in time. Formally, we expand the redundancy rate in the frequency domain as

$$I_{X_{\alpha};Y}^{\square} = \frac{1}{2\pi} \int_{-\pi}^{\pi} i_{X_{\alpha};Y}^{\square}(\omega) d\omega, \quad (5)$$

where i_{\cdot}^{\square} is the *spectral redundancy rate* defined at each normalized angular frequency $\omega \in [-\pi, \pi]$ according to the minimum MI principle [15] applied to the spectral MIR terms indexed by $\alpha = \{\alpha_1, \dots, \alpha_J\}$, i.e.

$$i_{X_{\alpha};Y}^{\square}(\omega) = \min_{j=1, \dots, J} i_{X_{\alpha_j};Y}(\omega). \quad (6)$$

In the case of two sources, the spectral redundancy rate corresponds to the individual spectral MIR terms

for the unique atoms (i.e., $i_{X_{\{k\}}^{\square};Y}(\omega) = i_{X_k;Y}(\omega)$, $k = 1, 2$), to their minimum for the redundant atom (i.e., $i_{X_{\{1\}\{2\}}^{\square};Y}(\omega) = \min\{i_{X_1;Y}(\omega), i_{X_2;Y}(\omega)\}$), and to the overall spectral MIR for the synergistic atom (i.e., $i_{X_{\{12\}}^{\square};Y}(\omega) = i_{X_1, X_2;Y}(\omega)$). Each spectral MIR is computed from the elements of the power spectral density of the joint process $S = \{X, Y\} = \{X_1, \dots, X_N, Y\}$, defined as $P_S(\omega) = \mathfrak{F}\{R_S(k)\}$, with $R_S(k) = \mathbb{E}[S_{n-k}^T S_n]$ being the covariance of S [20]. For instance, if $N = 2$ the individual and joint spectral MIR functions are

$$\begin{aligned} i_{X_k;Y}(\omega) &= \frac{1}{2} \log \frac{P_{X_k}(\omega) P_Y(\omega)}{|P_{[X_k Y]}(\omega)|}, k = 1, 2, \\ i_{X_1, X_2;Y}(\omega) &= \frac{1}{2} \log \frac{|P_{[X_1 X_2]}(\omega)| P_Y(\omega)}{|P_S(\omega)|}, \end{aligned} \quad (7)$$

where $P_{[X_k Y]}$ and $P_{[X_1 X_2]}$ are sub-matrices of the full spectral density P_S . Importantly, for Gaussian processes each spectral MIR is connected to its time-domain form by the spectral integration property (e.g., $I_{X_k;Y} = \frac{1}{2\pi} \int_{-\pi}^{\pi} i_{X_k;Y}(\omega) d\omega$) [20]. Exploiting this property, in [14] we show that there is a close connection between the spectral partial information and redundancy rates defined over a lattice structure identified at each frequency ω on the one side, and the time-domain partial information and redundancy rates defined here in (4) on the other side.

As an illustrative example of PIRD, we consider a simple network system whose connections are mapped by the vector random process $S = \{X_1, X_2, Y\}$ with dynamics determined by the stochastic equations

$$\begin{aligned} X_{1,n} &= a_1 X_{1,n-1} + b_1 X_{2,n-1} + U_{1,n}, \\ X_{2,n} &= a_2 X_{2,n-1} + b_2 X_{1,n-1} + U_{2,n}, \\ Y_n &= c_1 X_{1,n-1} + c_2 X_{2,n-1} + W_n, \end{aligned} \quad (8)$$

where W and U_k ($k = 1, 2$) are white and stationary innovation processes formed by i.i.d. standard Gaussian variables ($W_n, U_{k,n} \sim \mathcal{N}(0, 1)$) with covariances $R_{U_1 U_2} = \mathbb{E}[U_{1,n} U_{2,n}]$ and $R_{W U_k} = \mathbb{E}[W_n U_{k,n}]$. As depicted in Fig. 1a, the source processes X_1 and X_2 present internal dynamics modulated by the coefficients a_1, a_2 (orange arrows), and causal interactions are set between the sources and towards the target Y via the coefficients b_1, b_2 and c_1, c_2 (green arrows); all time-delayed interactions occur at lag 1, while instantaneous (non-delayed) interactions are determined by the innovation covariances (red dashed arrows).

The system (8) is analyzed by computing both PID and PIRD as a function of a modulation parameter $d \in [0, 1]$ that acts on the strength of instantaneous and time-lagged effects. First, we study (8) in the absence of instantaneous effects ($R_{U_1 U_2} = R_{W U_k} = 0$), letting the strength of causal interactions to increase progressively ($c_1 = c_2 = d$), and the strength of internal dynamics to decrease progressively ($a_1 = a_2 = 0.8(1 - d)$), with fixed coupling between the sources ($b_1 = b_2 = 0.1$). The analysis (Fig. 1b) documents that the target shares information at lag zero with the sources as soon as causal interactions are set ($I(Y_n; X_n) > 0$ when $d > 0$) even if instantaneous effects are kept to zero; this information does not exhibit a monotonic trend, and the PID suggests that it is seen as prevalently redundant ($R(Y_n; X_n) > S(Y_n; X_n)$). On the other hand,

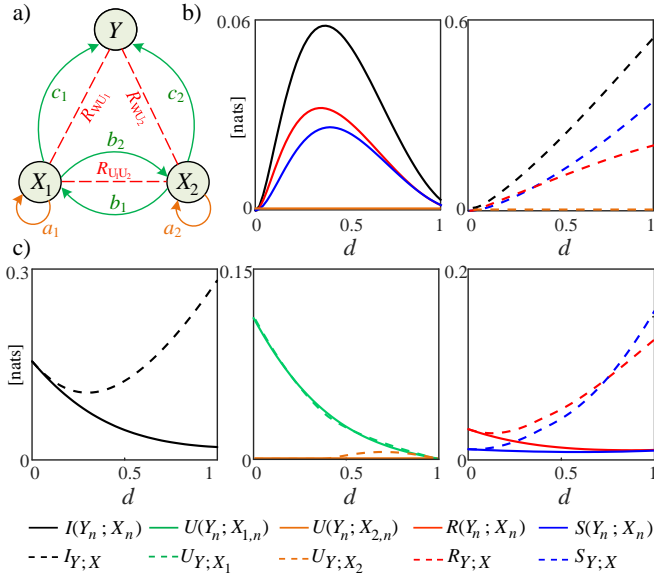


Figure 1. Decomposition of the multivariate information shared instantaneously and dynamically in a network Gaussian system (a) with instantaneous (red) and time-lagged (internal: orange; causal: green) simulated interactions. In the absence of instantaneous effects, the zero-lag multivariate information is modulated non-trivially by time-lagged effects and is predominantly redundant (b, left), while the dynamic information reflects the strength of time-lagged effects and is predominantly synergistic (b, right). When a transition from pure instantaneous to pure time-lagged effects is simulated (c), PID (solid lines) fails in detecting the trend and nature of multivariate interactions, while PIRD reveals the expected emergence of dynamic coupling (dashed, black) and net synergy (dashed, blue vs. red).

the PIRD captures the increasing rate of information shared by the target and source processes, and documents the emergence of net synergy consequent to the increased strength of the common child relations $X_1 \rightarrow Y$ and $X_2 \rightarrow Y$; the unique terms are null in this simulation where the two sources contribute equally to the target. In the second simulation setting, the system is investigated reproducing a transition from purely instantaneous to exclusively time-lagged interactions among the processes, achieved decreasing progressively the strength of zero lag effects ($R_{U_1 U_2} = R_{W U_2} = 0.25(1-d)$, $R_{W U_1} = 0.5(1-d)$) while increasing the strength of internal dynamics and causal interactions ($a_1 = a_2 = 0.2d$, $b_1 = b_2 = 0.1d$, $c_1 = c_2 = 0.6d$). The results in Fig. 1c confirm that the PIRD reduces to the PID in the absence of time-lagged effects ($d = 0$), but the injection of temporal correlations into the processes makes the two approaches to differ substantially: whilst the information shared between Y_n and $\{X_{1,n}, X_{2,n}\}$ decreases progressively together with its unique, redundant and synergistic contributions, the overall information rate between Y and $\{X_1, X_2\}$ initially decreases due to diminishing unique contribution of X_1 and then increases substantially due to the rise of both redundant and synergistic effects; net synergy emerges for $d > 0.7$, and the unique terms are both nonzero for $d > 0.5$.

As an application to real data, we consider an exemplary case study in climate science, i.e. the network of interactions among the most representative in-

stances descriptive of El Niño and the Southern Oscillation (ENSO). ENSO is a periodic fluctuation in the sea surface temperature and air pressure of the atmosphere overlying the equatorial Pacific Ocean, which is considered as the most prominent interannual climate variability on Earth [21]. Since the exact initiating causes of an ENSO warm or cool events are not fully understood, it is important to analyze the statistical relation between its two main components, i.e., atmospheric pressure and sea surface temperature. Such components are measured respectively by NINO34 (the East Central Tropical Pacific sea surface temperature anomaly, also called El Niño) and SOI (Southern Oscillation Index, the standardized difference in surface air pressure between Tahiti and Darwin), and are dynamically related to several other indexes that represent large scale climate patterns [22, 23]. The resulting network of causal interactions is densely connected through several feedback loops of inter-annual variations [23], suggesting the importance of studying high-order interactions with a comprehensive dynamic approach. Here, in addition to NINO34 and SOI we considered three more indices which can have a remarkable impact on ENSO as a result of high-order effects, i.e. TSA (Tropical Southern Atlantic Index), PDO (Pacific Decadal Oscillation), and NTA (North Tropical Atlantic) [24].

The analyzed climate indices are taken from a public database [23], of which we consider the series SOI, NINO34, TSA, PDO and NTA measured with a monthly sampling rate during the period 1950-2016 (792 data points) for which all time series values are available. The series were detrended and deseasonalized, and then analyzed under the assumption of Gaussianity so as to identify the terms relevant to the PID and PIRD formulations (the Gaussian assumption was adopted also in [23, 24]). The series were analyzed in triplets, considering SOI as the target and all possible pairs of other series as sources; for each triplet, PIRD and zero-lag PID were computed respectively from the parameters of a vector autoregressive (VAR) model [25] (least squares estimation, model order set according to the Akaike information criterion [26]) and a linear regression model identified on the three series (least squares estimation). To assess the significance of temporal correlations, the PIRD was computed both on the original time series and on surrogate series for which the static MI was preserved (random shuffling of the samples of each series, with the same random permutation applied to all series). We find that the pairs of sources including NINO34 share the highest amounts of information with the target SOI (Fig. 2a), and that such information arises from a unique contribution of NINO34 (Fig. 2b); unique effects are noticeable also when considering NTA (X_2 in the triplets 3,5,6, Fig. 2b). The index NTA contributes significantly also to high-order interactions (both redundant and synergistic, triplets 3,5,6 in Fig. 2c). Crucially, the importance of NTA is elicited only using PIRD and, more generally, surrogate data demonstrates that temporal correlations play a fundamental role in information decomposition and cannot be disregarded. These results confirm the main role played by El Niño temperature anomalies on atmospheric pressure and ENSO dynamics [23, 24], and documents the presence of dynamic many-body ef-

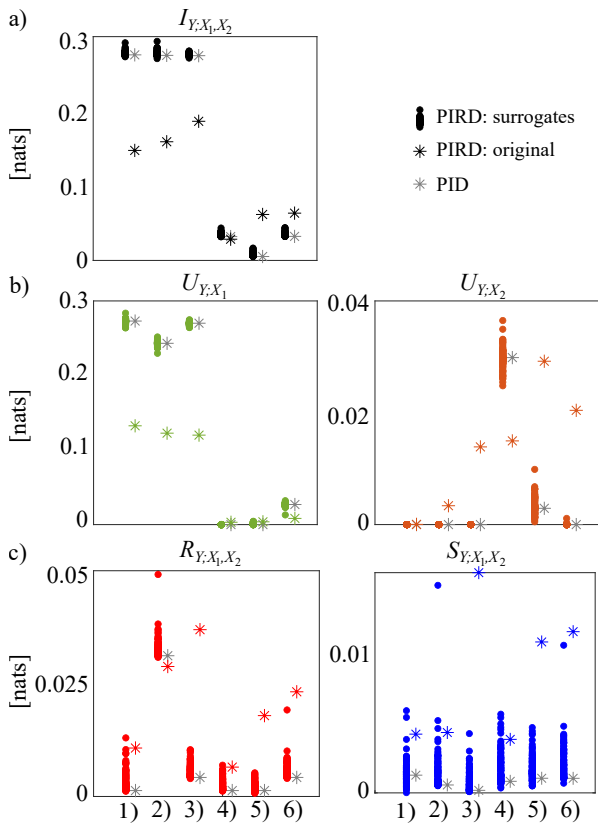


Figure 2. Decomposition of the multivariate information shared instantaneously and dynamically in six triplets of climate time series (target Y : SOI; sources $\{X_1, X_2\}$: 1) $\{NINO34, TSA\}$, 2) $\{NINO34, PDO\}$, 3) $\{NINO34, NTA\}$, 4) $\{TSA, PDO\}$, 5) $\{TSA, NTA\}$, 6) $\{PDO, NTA\}$). For each triplet, the multivariate information (a) is decomposed into unique (b) and redundant/synergistic (c) components via static PID (gray asterisks) and via the proposed dynamic PIRD (black/colored asterisks); PIRD is applied also on 100 surrogate triplets obtained via random shuffling preserving zero-lag correlations (circles).

fects involving the north tropical atlantic climate mode and the ENSO components.

In summary, the proposed framework offers a novel comprehensive method to parcel out the information shared by dynamic network systems into amounts quantifying unique and high-order effects. We posit that this framework generalizes and unifies previous PID theories applied to multivariate time series, establishing a new approach for the analysis of complex networks that reconciles information-theoretic and dynamical systems perspectives. Indeed, as it explicitly takes the full temporal statistical structure of random processes into account, PIRD overcomes the intrinsic limitation of PID of being unable to deal with temporally correlated variables. Moreover, the proposed spectral formulation of PIRD based on redundancy rates defined in the frequency domain allows to decompose dynamic information considering predetermined oscillations with specific meaning for the analyzed dynamic network. We expect that these properties, together with the algorithmic reliability and low computational demand of the implementation proposed here for PIRD, will open new avenues for the analysis of real-world networks with dynamic oscillatory behavior.

DATA AND CODE AVAILABILITY

The code to simulate and analyze data is available at www.lucafaes.net/PIRD.html. Climate data as described in [23] can be downloaded at the NOAA website <https://psl.noaa.gov/data/climateindices/list/>.

ACKNOWLEDGMENTS

This work was supported by the project ‘‘HONEST - High-Order Dynamical Networks in Computational Neuroscience and Physiology: an Information-Theoretic Framework’’, Italian Ministry of University and Research (funded by MUR, PRIN 2022, code 2022YMH-NPY, CUP: B53D23003020006).

-
- [1] P. L. Williams and R. D. Beer, arXiv preprint arXiv:1004.2515 (2010).
- [2] M. Wibral, V. Priesemann, J. W. Kay, J. T. Lizier, and W. A. Phillips, *Brain and cognition* **112**, 25 (2017).
- [3] Z. Cang and Q. Nie, *Nature communications* **11**, 2084 (2020).
- [4] F. E. Rosas, P. A. Mediano, H. J. Jensen, A. K. Seth, A. B. Barrett, R. L. Carhart-Harris, and D. Bor, *PLoS computational biology* **16**, e1008289 (2020).
- [5] A. I. Luppi, P. A. Mediano, F. E. Rosas, N. Holland, T. D. Fryer, J. T. O’Brien, J. B. Rowe, D. K. Menon, D. Bor, and E. A. Stamatakis, *Nature Neuroscience* **25**, 771 (2022).
- [6] P. Wollstadt, S. Schmitt, and M. Wibral, *J. Mach. Learn. Res.* **24**, 1 (2023).
- [7] P. Dissanayake, F. Hamman, B. Halder, I. Sucholutsky, Q. Zhang, and S. Dutta, arXiv preprint arXiv:2411.07483 (2024).
- [8] J. W. Kay, J. M. Schulz, and W. A. Phillips, *Entropy* **24**, 1021 (2022).
- [9] T. F. Varley, O. Sporns, S. Schaffelhofer, H. Scherberger, and B. Dann, *Proceedings of the National Academy of Sciences* **120**, e2207677120 (2023).
- [10] T. F. Varley, M. Pope, J. Faskowitz, and O. Sporns, *Communications biology* **6**, 451 (2023).
- [11] L. Koçillari, M. Celotto, N. A. Francis, S. Mukherjee, B. Babadi, P. O. Kanold, and S. Panzeri, *Brain Informatics* **10**, 34 (2023).
- [12] A. I. Luppi, P. A. Mediano, F. E. Rosas, J. Allanson, J. Pickard, R. L. Carhart-Harris, G. B. Williams, M. M. Craig, P. Finoia, A. M. Owen, *et al.*, *Elife* **12**, RP88173 (2024).
- [13] T. E. Duncan, *SIAM Journal on Applied Mathematics* **19**, 215 (1970).
- [14] L. Sparacino, G. Mijatovic, Y. Antonacci, L. Ricci, D. Marinazzo, S. Stramaglia, and L. Faes, arXiv preprint arXiv:2502.04555 (2025).
- [15] A. B. Barrett, *Physical Review E* **91**, 052802 (2015).
- [16] R. A. Ince, *Entropy* **19**, 318 (2017).
- [17] A. J. Gutknecht, M. Wibral, and A. Makkeh, *Proceedings of the Royal Society A* **477**, 20210110 (2021).
- [18] D. A. Ehrlich, K. Schick-Poland, A. Makkeh, F. Lanfermann, P. Wollstadt, and M. Wibral, *Physical Review E* **110**, 014115 (2024).

- [19] C. Finn and J. T. Lizier, *Entropy* **20**, 297 (2018).
- [20] L. Sparacino, Y. Antonacci, G. Mijatovic, and L. Faes, arXiv preprint arXiv:2401.11327 (2024).
- [21] M. J. McPhaden, S. E. Zebiak, and M. H. Glantz, *science* **314**, 1740 (2006).
- [22] P. Chang, R. Saravanan, and L. Ji, *Geophysical Research Letters* **30** (2003).
- [23] R. Silini, G. Tirabassi, M. Barreiro, L. Ferranti, and C. Masoller, *Climate Dynamics* **61**, 79 (2023).
- [24] S. Stramaglia, L. Faes, J. M. Cortes, and D. Marinazzo, *Physical Review Research* **6**, L032007 (2024).
- [25] H. Lütkepohl, *New introduction to multiple time series analysis* (Springer Science & Business Media, 2005).
- [26] L. Faes, S. Erla, and G. Nollo, *Computational and mathematical methods in medicine* **2012**, 140513 (2012).